Thermal transport barrier in heliotron-type devices (Large Helical Device and Compact Helical System)

Cite as: Physics of Plasmas **7**, 1802 (2000); https://doi.org/10.1063/1.874001
Submitted: 11 November 1999 • Accepted: 13 December 1999 • Published Online: 19 April 2000

N. Ohyabu, A. Fujisawa, N. Ashikawa, et al.

Thermal transport barrier in heliotron-type devices (Large Helical Device and Compact Helical System)*

N. Ohyabu,† A. Fujisawa, N. Ashikawa,[a] P. deVries, M. Emoto, H. Funaba, M. Goto, Y. Hamada, H. Iguchi, K. Ida, K. Itoh, M. Isobe, H. Idei, S. Inagaki, N. Inoue, K. Ikeda,[a] S. Kado, S. Kubo, R. Kumazawa, K. Khlopenkov, O. Kaneko, K. Kawahata, A. Komori, T. Kobuchi,[a] S. Lee,[a] Y. Liang,[a] T. Minami, J. Miyazawa, S. Masuzaki, K. Matsuoka, T. Morisaki, S. Morita, S. Murakami, T. Mutoh, S. Muto, K. Narihara, Y. Nagayama, Y. Nakamura, H. Nakanishi, K. Nishimura, S. Nishimura, N. Noda, I. Nomura, T. Notake,[b] S. Okamura, S. Ohdachi, K. Ohkubo, Y. Oka, M. Osakabe, T. Ozaki, B. J. Peterson, R. O. Pavlichenko, A. Sagara, S. Sakakibara, R. Sakamoto, M. Sasao, K. Sato, H. Sanuki, K. Saito,[b] M. Sato, T. Seki, A. Shimizu,[b] T. Shimozuma, M. Shoji, H. Suzuki, S. Sudo, H. Sasao,[a] Y. Takeiri, K. Tanaka, K. Toi, T. Tokuzawa, K. Tsumori, K. Tsuzuki, M. Takechi,[b] N. Tamura,[a] Y. Torii,[b] I. Yamada, H. Yamada, S. Yamaguchi, K. Yamazaki, M. Yokoyama, Y. Yoshimura, S. Yamamoto,[b] K. Y. Watanabe, T. Watanabe, T. Watari, O. Motojima, M. Fujiwara
National Institute for Fusion Science, Toki, Gifu-ken, 509-5292, Japan

(Received 11 November 1999; accepted 13 December 1999)

In the discharges of the Large Helical Device [O. Motojima *et al.*, *Proceedings of the 16th Conference on Fusion Energy*, Montreal, 1996 (International Atomic Energy Agency, Vienna, 1997), Vol. 3, p. 437], a significant enhancement of the energy confinement has been achieved with an edge thermal transport barrier, which exhibits a sharp gradient at the edge. Key features associated with the barrier are quite different from those seen in tokamaks (i) almost no change in particle (including impurity) transport, (ii) a gradual formation of the barrier, (iii) a very high ratio of the edge temperature to the average temperature, (iv) no edge relaxation phenomenon. In the electron cyclotron heating (ECH) heated discharges in the Compact Helical System [K. Matsuoka *et al.*, in *Proceedings of the 12th International Conference on Plasma Physics and Controlled Nuclear Fusion Research*, Nice, France, 1988 (International Atomic Energy Agency, Vienna, 1989), Vol. 2, p. 411], the internal electron transport barrier has been observed, which enhances the central electron temperature significantly. High shear of the radial electric field appears to suppress the turbulence in the core region and enhance the electron confinement there. © *2000 American Institute of Physics.* [S1070-664X(00)90905-4]

I. INTRODUCTION

The Large Helical Device (LHD) is a large heliotron type device with a divertor [$l=2$, $m=10$, R_{ax} (position of magnetic axis)$=3.6$–3.9 m, a (minor radius)$=0.6$ m, $B=3$ T].[1–4] The LHD experiment began in March 1998 after its 8 year construction. The major goal of the LHD experiment is to demonstrate high performance of a helical plasma in a reactor relevant plasma regime. The Compact Helical System (CHS) is a small version of the LHD [$l=2$, $m=8$, R_{ax} (position of the magnetic axis)$=1.0$ m, a (minor radius) $=0.2$ m, $B=2$ T], which has been operating since 1988.[5] Its data have provided physics guidance to the design and start-up of the LHD experiment. As in the other toroidal confinement systems, confinement degradation at higher input power is the major concern for our research.

In tokamak *H*-mode (high confinement mode) discharges, the edge thermal transport barrier suddenly appears when the input power exceeds a critical value, generating sharp temperature and density gradients (pedestal) just inside of the last closed magnetic surface (LCMS) and then leading to a factor of up to 2 enhancement of the energy confinement.[6] We have achieved a significant enhancement of the global energy confinement with an edge thermal transport barrier in the LHD discharges.[7] The key observed features of the LHD barrier, as described in the following section are quite different from those observed in tokamaks.[6,8] In smaller helical devices such as W7-AS (the Wendelstein VII-AS advanced stellarator)[9] and CHS,[10] *H*-mode has been observed, evidenced by steeping of the edge temperature and density profiles, a rapid drop in H_α and appearance of ELMs (edge localized modes).

More recently, an internal thermal transport barrier has been observed in the reverse shear configuration of the tokamak, leading to very significant enhancement of the energy confinement.[11–13] Maintaining such configuration stably is the major issue in the advanced tokamak program. In CHS,[14] a sharp gradient of T_e (internal electron transport barrier) at ρ (the normalized radius)$=0.25$ has also been observed in

*Paper LI21 Bull. Am. Phys. Soc. **44**, 220 (1999).
†Invited speaker.
[a]Graduate University for Advanced Studies, Hayama, 240-0193, Japan.
[b]Department of Energy Engineering and Science, Nagoya University 464-8603, Japan.

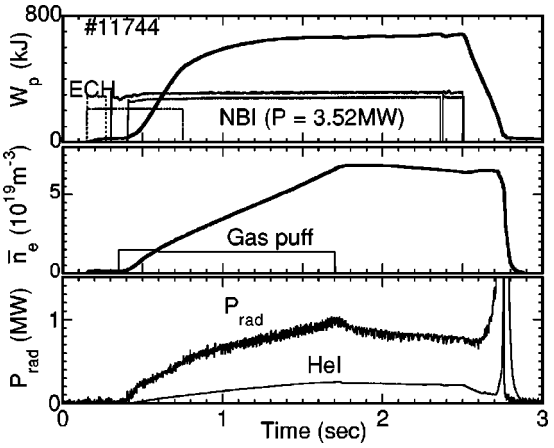

FIG. 1. Temporal evolution of a typical LHD discharge. W_p is the total stored plasma energy. P_{rad} is the total radiation power measured by a bolometric system.

the low density, electron cyclotron heating (ECH) heated discharges. In this paper, the edge and internal transport barriers observed in the heliotron type devices (LHD and CHS) are described.

II. EDGE TRANSPORT BARRIER IN THE LHD DISCHARGES

In the tokamak discharges, the edge confinement suddenly improves after a so called $L-H$ transition [L(low confinement) mode to H-mode transition], forming the temperature and density pedestals.[6,8] On the other hand, the pedestal in the LHD discharge forms during the rising phase, not through a rapid transition. Figure 1 shows temporal evolution of a typical LHD discharge. An ECH generated, small target plasma is heated by a neutral beam injection [P(input power) $=1$–4 MW]. With beam heating on, the hot plasma region expands radially and eventually reaches the LCMS and divertor plates. During this process, T_e^{ped} (the electron temperature at the shoulder of the pedestal, $\rho=0.85$–0.9) increases naturally, forming an edge temperature pedestal. The stored energy (W_p), density (n), and radiative power reach steady state levels after the gas puff off. There is no indication that the particle (including the impurity ions) confinement enhances significantly as in the H-mode. The electron temperature profile [$T_e(r)$] is measured by the Thomson scattering along the major radius (R) (at $Z=0$) at the poloidal plane where the plasma is elongated horizontally [Fig. 2(a)]. In Figs. 3–5, T_e profiles for various plasma parameters are plotted as a function of ρ. Clear pedestals with shoulder temperatures (T_e^{ped}) of 0.2–1.3 keV can been seen. The estimated total thermal conductivity ($n_e\chi$) there is fairly low, typically 1.0–$2.0\times10^{19}\,\mathrm{m^{-1}\,s^{-1}}$ and thus transport in this edge region can be called an edge thermal transport barrier. Here we assume that $T_e(r)=T_i(r)$ (the ion temperature). Presently, the T_i profile in the region $0.3<\rho<0.9$ for the low density discharges is available by CXR measurement and is found to be close to $T_e(r)$.

Most of the electron temperature profiles in the LHD discharges are approximately close to a model profile, shown

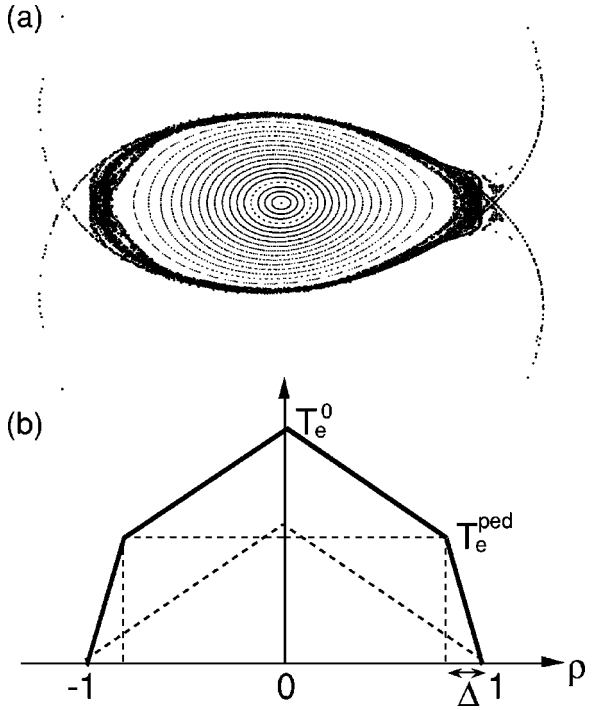

FIG. 2. (a) The LHD magnetic configuration. The T_e profile is measured along the major radius (R axis) ($Z=0$) by the Thomson scattering. (b) A model T_e profile for LHD discharges. A profile shown by dotted lines is a hypothetical one without pedestal.

in Fig. 2(b), characterized by two lines, i.e., core and edge lines. The edge temperature gradient ($T_e^{\mathrm{ped}}/\Delta$) is typically four times greater than that of the core [$(T_e^0-T_e^{\mathrm{ped}})/(1-\Delta)$]. Figure 3 shows profiles with two somewhat extreme plasma parameters [(a) one of the highest stored energy discharge, $W_p=760$ kJ, $n=6.3\times10^{19}\,\mathrm{m^{-3}}$, $B=2.75$ T, (b) one of the highest $\langle\beta\rangle$ discharge, $\langle\beta\rangle=1.3\%$, $n=2.3\times10^{19}\,\mathrm{m^{-3}}$, $B=0.75$ T]. The shape of the T_e profile, however, is nearly identical. For the low density discharges, the pedestal temperature becomes as high as 1.2 keV as shown in Fig. 4.

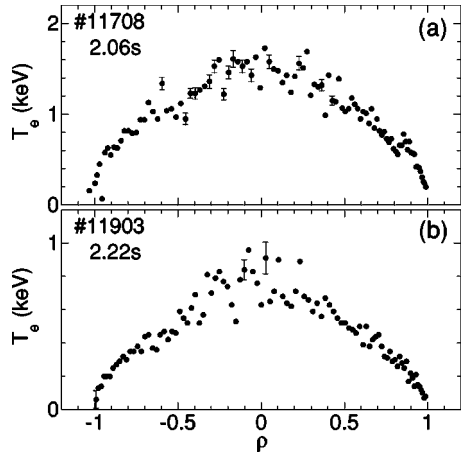

FIG. 3. (a) Temperature profile for high plasma pressure discharge ($R_{\mathrm{ax}}=3.6$ m, $B=2.75$ T, $P=3.4$ MW, $n_e=6.3\times10^{19}\,\mathrm{m^{-3}}$). (b) Temperature profile for high β discharge ($R_{\mathrm{ax}}=3.6$ m, $B=0.75$ T, $P=2.4$ MW, $n_e=2.3\times10^{19}\,\mathrm{m^{-3}}$).

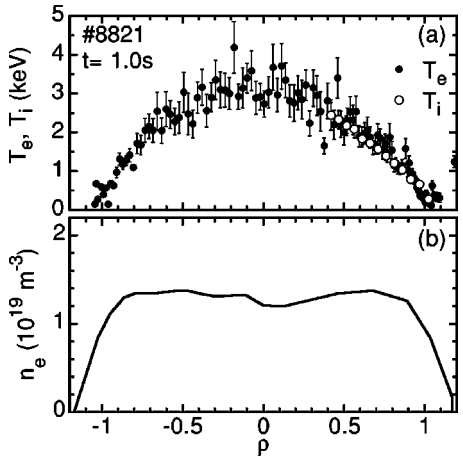

FIG. 4. Profiles for the high temperature discharges (R_{ax}=3.6 m, B =2.75 T, P=3.9 MW, n_e=1.6×10^{19} m^{-3}). The density profile measured by an array of the far infrared (FIR) laser interferometer.

The width of the pedestal (Δ) averaged over the flux surface is found to be 4–6 cm, which is much wider than that of the comparable tokamak. In the model profile, the average temperature ($\langle T_e \rangle$) with Δ=0.15 is given by $\langle T_e \rangle = 0.85\, T_e^{\rm ped} + 0.24\ (T_e^0 - T_e^{\rm ped})$. One of the amazing features of the LHD edge barrier is that the pedestal temperature is found to be close to the average temperature ($\langle T_e \rangle$) [the temperature ratio ($T_e^{\rm ped}/\langle T_e \rangle$) can be as high as 0.8]. Thus W_p is almost proportional to $n_e\ T_e^{\rm ped}$ and hence the edge confinement almost determines τ_E (the global energy confinement time). To study dynamic behavior of the T_e profile,

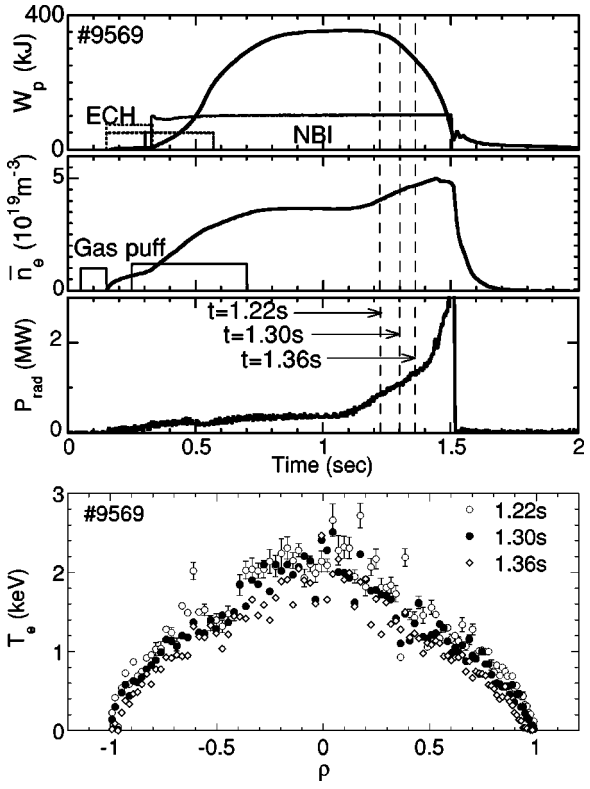

FIG. 5. Evolution of the temperature profile after injection of a large amount of neon gas (R_{ax}=3.6 m, B=2.75 T, P=1.6 MW).

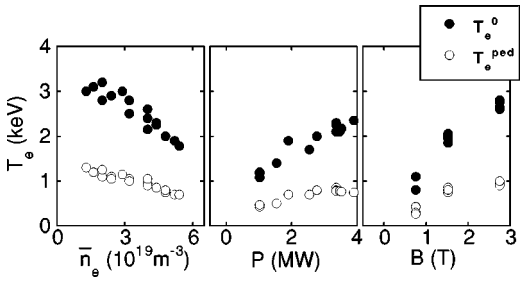

FIG. 6. Parametric dependencies of T_e^0 and $T_e^{\rm ped}$. Dependencies of T_e^0 and $T_e^{\rm ped}$ on the average density (n_e). (R_{ax}=3.6 m, B=2.75 T, P=3.3 MW). Dependencies of T_e^0 and $T_e^{\rm ped}$ on power (P). (R_{ax}=3.6 m, B=2.75 T, n_e =4.4×10^{19} m^{-3}). Dependencies of T_e^0 and $T_e^{\rm ped}$ on the magnetic field strength (B). (R_{ax}=3.6 m, P=2.3 MW, n_e=2.0×10^{19} m^{-3}).

we inject the neon gas during the middle of the discharge. The neon impurity radiation becomes high only in the edge region, but the whole temperature profile drop simultaneously, preserving the model profile. This suggests existence of some nonlocal transport mechanism, which could dominate the heat transport in the LHD.

The density dependencies of T_e^0 and $T_e^{\rm ped}$ (at the fixed input power) are depicted in Fig. 6(a). Both central and pedestal temperatures decrease gradually with increasing density, leading to higher stored energy at higher density. When n is below 3×10^{19} m^{-3}, $T_e^{\rm ped}$ exceeds 1 keV. Figure 6(b) shows power dependencies of T_e^0 and $T_e^{\rm ped}$ for a fixed density ($n \sim 4.4\times10^{19}$ m^{-3}). Both temperatures increase rapidly with input power when P is below 2 MW. In higher power regime, however, the increment of $T_e^{\rm ped}$ with power is modest. This is the main issue, which we have to solve experimentally. Optimistically, further higher power in the near future experiment could naturally lead to the better confinement regime or mode. We are also considering a more drastic edge control by combination of the pellet or beam fueling and high efficient pumping. As in tokamak transport, the temperatures increase approximately linearly with magnetic field [Fig. 6(c)].

The LHD density profile is generally very flat, mostly with a very modest inversion of the density gradient [Fig. 4(b)]. Since the density is nearly zero at the very edge, there is a relatively sharp density gradient. But a high density gradient exists outside of the LCMS (ρ=1) where the electron temperature is kept low by the electron parallel heat transport. This means that particle confinement almost takes place in the open ergodic region, which surrounds the confining region[15] [see Fig. 2(a)]. This is not surprising since cold ions are well confined in the open edge region where the connection length is longer than 300 m. This is quite a contrast to the *H*-mode barrier, which is characterized by a very sharp density gradient due to a nearly perfect particle transport barrier. For the inward shifted configuration (R_{ax}=3.60 m), the ergodic layer regions are much narrower compared with that with R_{ax}=3.70 m, thereby being closer to that of the tokamak configuration with a sharp separation of the closed and open regions. This results in a fair overlapping of the high ∇T_e and high ∇n_e regions, which is believed to be a

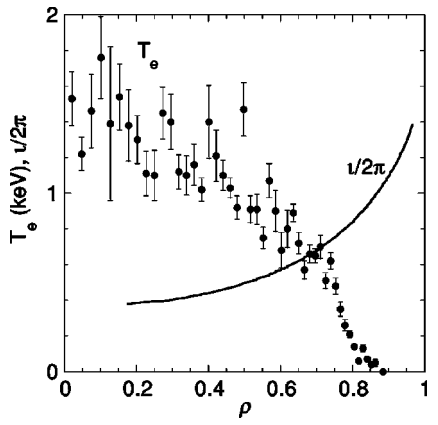

FIG. 7. The pedestal is seen at $\rho=0.75$ during the rising phase of low density discharge ($n_e=0.8\times10^{19}\,\mathrm{m}^{-3}$, $B=2.5\,\mathrm{T}$, $R_{\mathrm{ax}}=3.60\,\mathrm{m}$). The $\iota/2\pi=1$ surface is located at $\rho=0.87$.

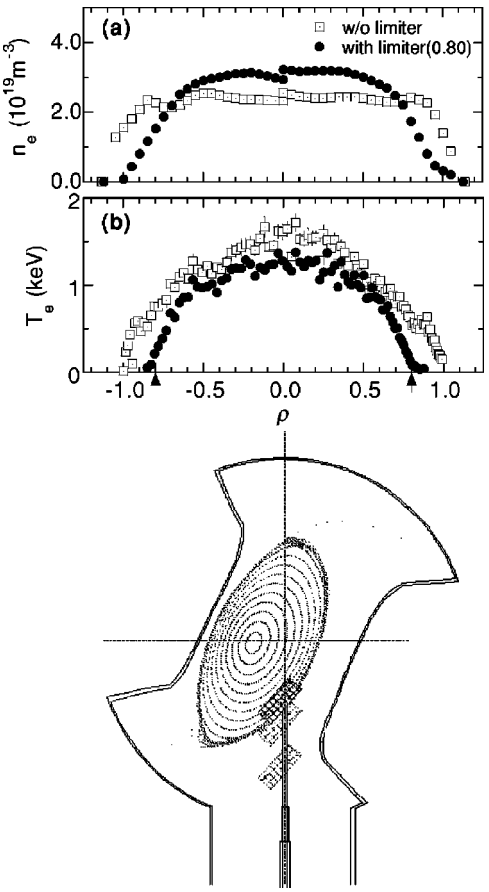

FIG. 8. Pedestal in the LHD limiter discharge ($B=2.75\,\mathrm{T}$, $R_{\mathrm{ax}}=3.60\,\mathrm{m}$, $P=1.5\,\mathrm{MW}$). The geometry of the limiter is depicted. The density profiles (a) and temperature profiles (b) with and without limiter are shown. The normalized radius (ρ) is defined for the discharge without limiter. The location of the limiter leading edge is $\rho=0.8$.

favorable condition for confinement enhancement. Indeed this configuration exhibits a factor of ~30% improvement of τ_E over the configurations with larger $R_{\mathrm{ax}}(=3.70\,\mathrm{m})$. (But the improvement could be due to other reasons, e.g., better particle orbit properties in this configuration may reduce the anomalous transport). The *H*-mode discharges with perfect particle transport barrier suffer a continuous rise of the density and impurity concentration during the edge localized mode (ELM) free phase of the *H*-mode, eventually leading to radiative collapse. No improvement in the particle confinement for the LHD discharge avoids such a problem.

The edge temperature and density at the pedestal shoulder are comparable to those of the comparable tokamaks, but the edge pressure gradient is lower due to wider pedestal width. For high β (~1%) discharges, the normalized pressure gradient defined as $\nabla p_N=a\nabla P/(B^2/2\mu)$ becomes as high as 0.06 at the middle of the steep gradient, which is still below the Mercier stability limit due to high shear at the edge. In the core region, on the other hand, ∇P is milder, i.e., a factor of 4 lower, but Mercier stability condition is violated [we, however, did not observe any magnetohydrodynamics (MHD) activity which influences the transport so far]. In the tokamak *H*-mode, ELMs appear repetitively, expelling a fraction of the particle and energy to the divertor plates in a short time. It has been argued that an ELM is a relaxation (MHD) phenomenon caused by ballooning mode, which becomes unstable when the pressure gradient exceeds a critical value.[16] For the DIII-D tokamak discharge ($Ip=1.25\,\mathrm{MA}$, $B=2.1\,\mathrm{T}$ with an assumption of $T_e=T_i$),[16] the observed critical normalized pressure gradient prior to the occurrence of an ELM is 0.11, higher than the maximum value achieved in LHD to date. In the LHD discharges, the maximum average β value attained to date is 1.36% and we have not seen any relaxation phenomenon which influences the transport of the plasma so far.

In smaller helical devices,[9,10] the edge transport barrier (*H*-mode) has been observed only when the LCMS is close to the major rational surface with $\iota/2\pi$ (the rotational transform)=1 or 0.5. For the LHD discharges, the sharp temperature gradient normally appears at the edge. The $\iota/2\pi=1$ surface and a small $m/n=1/1$ island (generated by an error field and seen clearly in the T_e profile under some conditions) are located in the edge ($0.85<\rho<1.0$) for the configurations used in the LHD experiment, including the limiter discharge (described below) and thus the location of the high ∇T_e region can be interpreted to be around the $\iota/2\pi=1$ surface. Furthermore, a clear pedestal also appears around $\rho\approx0.75$, deeply inside the LCMS only during the plasma expanding phase of the low density discharge with $R_{\mathrm{ax}}=3.6\,\mathrm{m}$ and $B=2.5\,\mathrm{T}$ (Fig. 7). But we also note that the high gradient region is close to the $\iota/2\pi=1$ surface. Thus the $m/n=1/1$ island or $\iota/2\pi=1$ surface is likely to play some role in the formation of the edge thermal transport barrier in LHD.

To study the mechanism of the barrier formation, we inserted a small limiter,[17] a carbon plate into the core plasma, up to $\rho=0.8$ surface, as illustrated in Fig. 8. The limiter does limit the hot plasma, but it does not limit the cold plasma sharply. With limiter in, the hot plasma region shrinks and the stored energy becomes nearly half. But the barrier still exists and the temperature gradient remains almost unchanged. This demonstrated that neither the helical divertor configuration nor the ergodic magnetic structure play a major role in the formation of the LHD barrier. The small radial scale length of the density, possibly a key factor for the

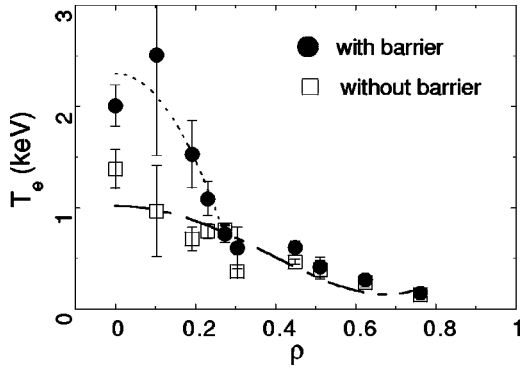

FIG. 9. Electron temperature profiles for the CHS discharges with and without barrier. The line averaged densities are $n_e=0.4\times10^{19}\,\mathrm{m}^{-3}$ and $n_e=0.3\times10^{19}\,\mathrm{m}^{-3}$ for the cases with and without barrier, respectively (Ref. 14).

tokamak *H*-mode transport barrier is not important either because it is very long in the barrier region for the LHD case, particularly for the limiter configuration.

III. INTERNAL ELECTRON TRANSPORT BARRIER IN CHS

In the CHS device, an internal transport barrier for electrons is found in rather strong ECR-heated plasmas where the axis magnetic field strength is 0.88 T.[14] The gyrotron frequency of 53.2 GHz has a resonance exactly on the axis. Figure 9 presents electron temperature T_e profiles with (closed circles) and without (squares) the internal transport barrier. The applied ECH-heating power and the line-averaged density are $P_{\mathrm{ECH}}=200\,\mathrm{kW}$, $n_e=0.4\times10^{19}\,\mathrm{m}^{-3}$, and $P_{\mathrm{ECH}}=150\,\mathrm{kW}$, $n_e=0.3\times10^{19}\,\mathrm{m}^{-3}$ for the cases with and without barrier, respectively. The central electron temperature with a barrier is 2.0 ± 0.2 keV, while that without barrier is 1.4 ± 0.1 keV. The T_e-profiles outside the normalized radius of $\rho=0.25$ are almost the same for both states. The clear difference in the temperature profile is seen within $\rho=0.25$.

Potential profiles and density fluctuation around the barrier are measured using the heavy ion beam probe (HIBP) for ECH heated plasmas with and without barrier. Figure 10 shows a typical example of the measurements with a spatial resolution of 2 mm. The potential profile indicates a clear change of its gradient at the barrier location of $\rho=0.25$. The electric field can be expressed by a form of $\tanh[(\rho-\rho_0)/\alpha]$. By fitting the integrated form to the measured potential slope around the barrier, as is shown in Fig. 10(a), the fine structure of radial electric field is deduced. Figure 10(b) shows the radial electric field and its shear as a function of normalized minor radius. The E_r-values inside and outside the barrier are 7.8 ± 0.7 kV/m and 1.7 ± 0.3 kV/m, respectively. In real dimension, the full-width at half-maximum and the barrier position from the plasma center are 1.3 ± 0.5 cm and 4.7 ± 0.4 cm, respectively. The resulting E_r-shear is $\sim39.7\pm17.4$ V/cm^2.

The fluctuation reduction is also confirmed at the transport barrier or the E_r-shear maximum radius. Figure 10(c) shows integrated power of density fluctuation spectrum

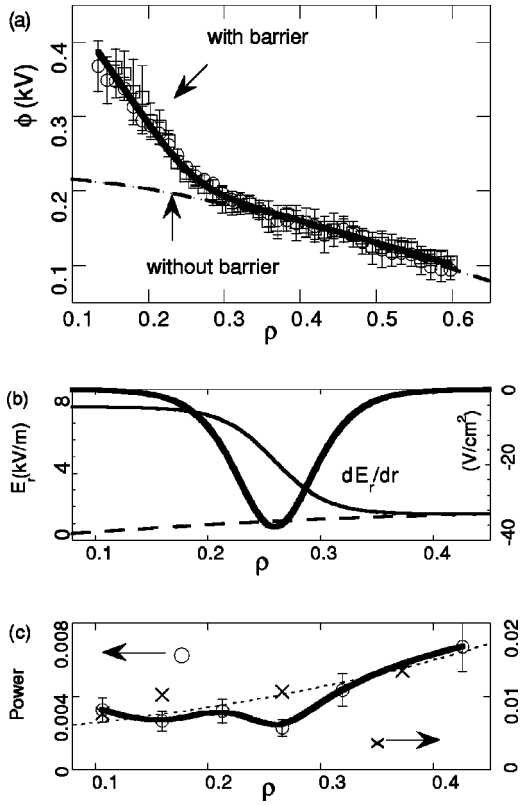

FIG. 10. Precise measurements around the barrier location using a HIBP in CHS. (a) Fine structure of potential around the barrier point. Here two data sets from sequential shots are plotted, and used for the fitting process. (b) Deduced E_r-structure and its shear. Profiles of potential and E_r without barrier are shown as reference. (c) Integrated fluctuation powers. The circles and crosses represent those of states with and without transport barriers, respectively (Ref. 14).

around the barrier. The integral is performed from 5 kHz to 70 kHz. Since the power spectrum above 70 kHz just shows the nature of *white noise* owing to path integral effects. In Fig. 10(c) the fluctuation power is obviously reduced at the barrier. The reduction of fluctuation power at the shear-maximum point is 48% if the integral fluctuation level subtracted by the noise is used for the estimation. Therefore, the reduction should lead to lessening of the fluctuation-driven transport, and should contribute to the formation of an internal transport barrier.

IV. DISCUSSIONS

For the *H*-mode cases, enhancement of τ_E can be easily estimated by comparing the stored energies just before and well after the *H*-transition. For the LHD discharges, which do not exhibit any transition, we consider a hypothetical T_e profile with the same $\partial T_e/\partial r$ as that observed in the core, but without pedestal, as shown by the dotted lines in Fig. 2(b). By comparing real and hypothetical profiles, we find that enhancement factor of τ_E is between 2 and 3. This is a significant enhancement. Such a comparison is justified from experimental observations. When excessive gas puffing or impurity injection cools the edge, the profile approaches one similar to the hypothetical one with a substantial reduction of τ_E, but such a profile is transient (Fig. 5). We have tested

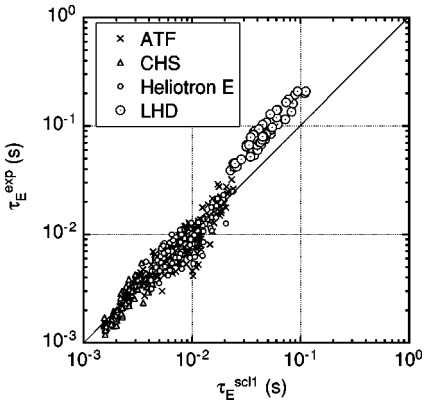

FIG. 11. Comparisons of LHD energy confinement times with the scaling (τ_E^{scl1}) based on the data from smaller heliotron type devices [Heliotron E; Advanced Toroidal Facility ATF and CHS] (Ref. 19).

configurations with various position of the axis (R_{ax}) from 3.6 m to 3.9 m. The enhancement factor appears to decrease with increasing R_{ax} and for the inward shifted configuration ($R_{ax}=3.6$ m) with good particle orbit properties exhibits a factor of 1.5 enhancement over the ISS95 (International Stellarator Scaling 1995).[18] Compared to the empirical scaling based on heliotron-type smaller devices (which is ~30% lower than the ISS95), the enhancement factor is ~2 (Fig. 11).[19] The enhancement over the scaling is due to the edge transport barrier.

A model for the LHD edge barrier is the following: the LHD discharge is purely *L*-mode, but a very low q ($=2\pi/\iota$) value at the edge of the LHD configuration leads to a sharp temperature gradient there. The ISS95 scaling is consistent with τ_E of tokamak *L*-mode discharges, suggesting that the similar *L*-mode transport mechanism dominates the transport in both helical devices and *L*-mode tokamaks. Furthermore, the edge plasma behavior in the LHD discharges is more like those of the *L*-mode except for the existence of the high temperature pedestal. The thermal diffusivity is believed to be a function of the dimensionless plasma parameters, geometrical factor and q profile. Supposed that the thermal diffusivity in the tokamak *L*-mode increases strongly with increasing q value, lower $q(\approx 1)$ at the central region and higher q (typically 3–4) at the edge for the tokamak result in a fairly peaked temperature profile, as seen experimentally. One of the significant difference between the tokamak and heliotron type device is the q ($=2\pi/\iota$) profile. As depicted in Fig. 7, q-values at $\rho=0$ and $\rho=1$ for LHD are 1/0.4 and 1/1.6, respectively. With the same diffusivity, the LHD type q-profile leads to a sharp gradient at the edge and moderate gradient in the core. Such a q profile is advantageous in achieving higher stored energy and hence the higher energy confinement.

Another plausible model for the LHD edge pedestal is that $q=1$ surface or its associated island ($m/n=1/1$) could play a major role in formation of the edge pedestal. Circumstantial experimental evidence for this is described in Sec. II. In the LHD magnetic configuration, the neoclassical (ripple) particle loss determines the radial electric field (E_r) which is on the order of $\nabla T/e$ or $T\nabla n/en$ ($\nabla T/e \gg T\nabla n/en$ for LHD discharges). With an island, the temperature there is flattened and thus E_r there is forced to be zero. This makes $\partial E_r/\partial r$ large around the island. Large $\partial E_r/\partial r$, in turn suppresses the turbulence[20] and the confinement around the island improves, resulting in sharper gradients on the both sides of the $\iota/2\pi=1$ surface (experimentally, we found that the gradient in the outer side of the surface is higher than that in the inner side). The required island size for flattening of the temperature is a few cm at $T_e=500$ eV and it is much smaller than size of the island which naturally exists due to small misalignment of the coil or structure with magnetic material.

As to the internal transport barrier observed in CHS, the neoclassical transport theory explains the key part of the mechanism. The absolute value of E_r as well as the E_r-shear is important for transports, particularly in collisionless plasma in the helical devices. The strongly positive E_r (electron root) should have better neoclassical transport property than the slightly positive E_r (ion root). Hence, the transition of E_r to the strongly positive branch may potentially contribute to the formation of the internal transport barrier in toroidal helical plasmas. The formation mechanism of the presented internal transport barrier is associated with the bifurcation property of the radial electric field inherent with toroidal helical plasma.[21,22] Above the power threshold, the E_r near the core bifurcates into a strongly positive branch, with the radial electric field outside remaining in the weakly positive branch. A connection layer appears at a radial location where two E_r-branches converge. There, a strong E_r-shear is created in that layer if its width is sufficiently thin. Then, the internal transport barrier is formed owing to the reduction of the fluctuation driven transport and the neoclassical transport.

A peculiarity of the CHS transport barrier is that the density profile indicates no gradient change at the barrier location. This may be related to the importance of off-diagonal terms for the neoclassical particle flux in the toroidal helical plasma. The neoclassical calculation gives the particle fluxes of $\Gamma^{neo}\sim 0.2\times 10^{20}\,m^{-2}\,s^{-1}$ and $\Gamma^{neo}\sim 1.5\times 10^{20}\,m^{-2}\,s^{-1}$ at the barrier location for the states without and with barrier, respectively. In the state with barrier, a decrease in the fluctuation driven particle flux could compensate the neoclassical part enhanced by the T_e-gradient.

V. SUMMARY

In summary, we have achieved a significant improvement of the energy confinement with an edge thermal barrier. Key associated features of the LHD edge thermal barrier are quite different from those of *H*-mode discharges in tokamaks and helical devices, (i) formation of the barrier is gradual (vs sudden formation after the transition for the *H*-mode), (ii) almost no improvement of the particle (including impurity) confinement (in contrast to formation of the density pedestal and significant enhancement of the particle confinement for *H*-mode), (iii) a very high ratio of the edge temperature to the average temperature, (iv) no edge relaxation phenomenon so far (whereas high edge pressure gradient is subject to regular collapse for the *H*-mode, a potential obstacle in ap-

plication to a reactor grade device). The LHD thermal transport barrier is not a version of the *H*-mode since the key associated features are completely different. In the coming experimental phase, more detailed measurements are planned to clarify the mechanisms of the pedestal formation along with an attempt to achieve a higher pedestal temperature (a few keV) for further enhancement of the energy confinement in LHD.

In CHS, the internal electron transport barrier has been observed in ECH heated low density discharges. The HIBP measurement demonstrated existence of high E_r-shear at the barrier, which is explained by neoclassical transport theory. High E_r-shear appears to suppress the dominant turbulence (as evidenced by observed reduction of the turbulence), leading to enhancement of the core electron confinement.

[1]A. Iiyoshi, M. Fujiwara, O. Motojima, N. Ohyabu, and K. Yamazaki, Fusion Technol. **17**, 169 (1990).
[2]M. Fujiwara, K. Yamazaki, M. Okamoto *et al.*, J. Fusion Energy **15**, 7 (1996).
[3]A. Iiyoshi, A. Komori, A. Ejiri *et al.*, Nucl. Fusion **39**, 1245 (1999).
[4]O. Motojima, H. Yamada, A. Komori *et al.*, Phys. Plasmas **6**, 1843 (1999).
[5]K. Ida, H. Yamada, H. Iguchi *et al.*, Phys. Rev. Lett. **67**, 58 (1991); S. Okamura, K. Matsuoka, K. Nishimura *et al.*, Nucl. Fusion **35**, 283 (1995).
[6]F. Wagner, G. Becker, K. Behringer *et al.*, Phys. Rev. Lett. **49**, 1408 (1982).
[7]N. Ohyabu, K. Narahara, H. Funaba *et al.*, Phys. Rev. Lett. **84**, 103 (2000).
[8]K. H. Burrell, S. L. Allen, G. Bramson *et al.*, Plasma Phys. Controlled Fusion **31**, 1649 (1989).
[9]V. Erckmann, F. Wagner, J. Baldzuhn *et al.*, Phys. Rev. Lett. **70**, 2086 (1993).
[10]K. Toi, S. Okamura, H. Iguchi *et al.*, in *Proceedings of the 14th International Conference on Plasma Physics and Controlled Nuclear Fusion Research, Wurtzburg, 1992* (International Atomic Energy Agency, Vienna, 1993), Vol. 2, p. 461.
[11]F. M. Levinton, M. C. Zarnstorff, S. H. Batha *et al.*, Phys. Rev. Lett. **24**, 4417 (1995).
[12]E. J. Strait, L. L. Lao, M. E. Mauel *et al.*, Phys. Rev. Lett. **24**, 4421 (1995).
[13]T. Fujita, S. Idei, H. Shirai *et al.*, Phys. Rev. Lett. **78**, 2377 (1997).
[14]A. Fujisawa, H. Ichiguchi, T. Minami *et al.*, Phys. Rev. Lett. **82**, 2669 (1999).
[15]N. Ohyabu, T. Watanabe, H. Ji *et al.*, Nucl. Fusion **34**, 387 (1994).
[16]P. Gohil, M. Ali Mahdavi, L. Lao *et al.*, Phys. Rev. Lett. **61**, 1603 (1988).
[17]K. Nishimura (private communication, 1999).
[18]U. Stroth, M. Murakami, H. Yamada *et al.*, Nucl. Fusion **36**, 1063 (1996).
[19]H. Yamada, K. Y. Watanabe, S. Sakakibara *et al.*, Phys. Rev. Lett. **84**, 1216 (2000).
[20]H. Biglari, P. H. Diamond, and P. W. Terry, Phys. Fluids B **2**, 1 (1990).
[21]L. M. Kovrizhnykh, Nucl. Fusion **24**, 435 (1984).
[22]D. E. Hastings, W. A. Houlberg, and K. C. Shaing, Nucl. Fusion **25**, 445 (1985).